A cyanide-bridged wheel featuring a seven-coordinate Mo(III) center

ChemComm

A cyanide-bridged wheel featuring a seven-coordinate Mo(III) center†

David K. Kempe,[a] Brian S. Dolinar,[a] Kuduva R. Vignesh,[a] Toby J. Woods,[a,b] Mohamed R. Saber,[a,c] and Kim R. Dunbar[a]*

A new cyclic molecule incorporating [Mo^{III}(CN)$_7$]$^{4-}$ has been characterized by single crystal X-ray methods, SQUID magnetometry and theoretical calculations. The wheel molecule [Mo^{III}(CN)$_7$]$_6$[Ni(L)]$_{12}$(H$_2$O)$_6$ exhibits ferromagnetic Mo-Ni coupling which did not exist for the previously reported octacyanometallate analogue [Mo^{IV}(CN)$_8$]$_6$[Ni(L)]$_{12}$(H$_2$O)$_6$. These results indicate that known supramolecular architectures incorporating octacyanometallates can be used as platforms for making new molecules incorporating seven-coordinate cyanide precursors.

The discovery of magnetic bistability in Mn$_{12}$ acetate[1] in 1993 opened the door to wide exploration of magnetic behavior in molecular materials. Cyanide materials experienced a renaissance in this area owing to the discovery of fascinating magnetic properties in Prussian Blue analogues such as the material V^{II}[Cr^{III}(CN)$_6$]$_{0.86}$·2.8 H$_2$O, which exhibits magnetic ordering above room temperature.[2] Over the past twenty years, hexacyanometallates, octacyanometallates, as well as heteroleptic cyanide precursors have been studied extensively vis-à-vis their capacity to be incorporated into extended networks as well as discrete molecules.[3-5] In the latter category, single molecule magnets (SMMs) prepared from cyanometallate building blocks are especially intriguing due to their potential applicability to quantum computing, data storage, and spintronics.[6-9] SMMs function as nanomagnets with a thermal energy barrier to reversal of their magnetization. Even in cases with record coupling[10,11] and large ground state spin values,[12] however, SMM behavior is still relatively elusive in cyanide-bridged materials. Investigating underexplored geometries and architectures can aid in the understanding of including how to improve their magnetic properties.

Molecular wheels are well-known in the magnetism and coordination chemistry communities with many different bridging ligands having been used to obtain cyclic architectures. Among these wheels are examples that contain lanthanides and transition metals with a wide variety of bridging ligands including azides, carboxylates, polyolates, polyamines, oxides, polyols, and hydroxides.[13-21] Wheel examples with cyanide, however, are rather limited,[12,22-27] despite the interesting magnetic phenomena observed for some of those

compounds. One of these molecules, [Mn^{III}(salen)]$_6$[Fe^{III}(bpmb)(CN)$_2$]$_6$•7H$_2$O exhibits magnetic hysteresis consistent with SMM behavior.[23] Another interesting molecule reported by us, namely [Mn(dpop)(H$_2$O)$_2$]$_2$[{Mo(CN)$_7$}$_8${Mn(dpop)}$_{10}${Mn(dpop)(H$_2$O)}$_4$]·xH$_2$O (dpop = 2,13-dimethyl-3,6,9,12,18-pentaazabicyclo-[12.3.1]octadeca-1(18),2,12,14,16-pentaene), has the largest spin ground state for a cyanide bridged molecule .[12] Based on that result and the dearth of cyanide-bridged wheels, we decided to pursue other wheel architectures utilizing [Mo^{III}(CN)$_7$]$^{4-}$ as a building block.

The S = ½ anion [Mo^{III}(CN)$_7$]$^{4-}$ has attracted interest in the area of cyanide magnetism due to its five-fold symmetry and atypical coordination geometries in magnetic systems. Early studies by Kahn and coworkers focused on the incorporation of [Mo(CN)$_7$]$^{4-}$ into extended cyanide-bridged networks. The seven-coordinate geometry precludes the formation of the highly symmetric networks typically observed for hexa- and octacyanometallates and leads to increased magnetic anisotropy.[28,29] Examples of molecules containing the [Mo^{III}(CN)$_7$]$^{4-}$ moiety are scarce, however; results from our laboratories have provided the only examples that satisfy the conditions for SMMs, *viz.* the Mo^{III} center having pseudo-D$_{5h}$ geometry and a 3d metal being coordinated to the apical cyanide ligands which maximizes Ising anisotropy.[30-33] While one would not expect to preserve the D$_{5h}$ symmetry when incorporating [Mo^{III}(CN)$_7$]$^{4-}$ into wheel architectures, isolation of new cyclic molecules with this anion allows for more data to be added to the scarce information about the magnetism of this building block .

One family of wheels that incorporates homoleptic cyanometallates have the formula [M^{IV}(CN)$_8$]$_6$[Ni(L)]$_{12}$(H$_2$O)$_6$ (M = Nb, Mo, or W). Weak antiferromagnetic interactions between the Ni centers in [Mo^{IV}(CN)$_8$]$_6$[Ni(L)]$_{12}$(H$_2$O)$_6$[25] and antiferromagnetic interactions between Nb and Ni in [Nb^{IV}(CN)$_8$]$_6$[Ni(L)]$_{12}$(H$_2$O)$_6$ were reported in the original publications.[27] The magnetic properties of [W^{IV}(CN)$_8$]$_6$[Ni(L)]$_{12}$(H$_2$O)$_6$ were not reported.[26]

In this report, we describe the synthesis of the Mo^{III} analogue [Mo^{III}(CN)$_7$]$_6$[Ni(L)]$_{12}$(H$_2$O)$_6$ (**Mo$_6^{III}$Ni$_{12}$**) by emulating reaction conditions used to prepare [Mo^{IV}(CN)$_8$]$_6$[Ni(L)]$_{12}$(H$_2$O)$_6$ (**Mo$_6^{IV}$Ni$_{12}$**). We also prepared a sample of the **Mo$_6^{IV}$Ni$_{12}$** analogue to directly compare data for the two molecules and devised a new, simpler procedure for the synthesis of K$_4$[Mo^{III}(CN)$_7$]·2H$_2$O (see ESI for details).[34]

Mo$_6^{III}$Ni$_{12}$ was synthesized at room temperature by mixing aqueous solutions of K$_4$[Mo^{III}(CN)$_7$]·2H$_2$O and Ni(L)(ClO$_4$)$_2$ (L = (2E,11E)-2,12-dimethyl-3,7,11-triaza-1(2,6)pyridinacyclo-dodecaphane-2,11-diene). Thin, orange needles were harvested after the solution was left to stand undisturbed overnight. The **Mo$_6^{III}$Ni$_{12}$** compound crystallizes in P$\bar{1}$ with a unit cell that is metrically similar to that of **Mo$_6^{IV}$Ni$_{12}$**,

[a] Department of Chemistry, Texas A&M University, College Station, Texas 77842-3012, United States
Email: dunbar@chem.tamu.edu; Fax +1 979 845 7177
[b] George L. Clark X-Ray Facility and 3M Materials Laboratory, University of Illinois at Urbana-Champaign, 505 South Mathews Avenue, Urbana, IL 61801, USA.
[c] Chemistry Department, Faculty of Science, Fayoum University, Fayoum 63514, Egypt
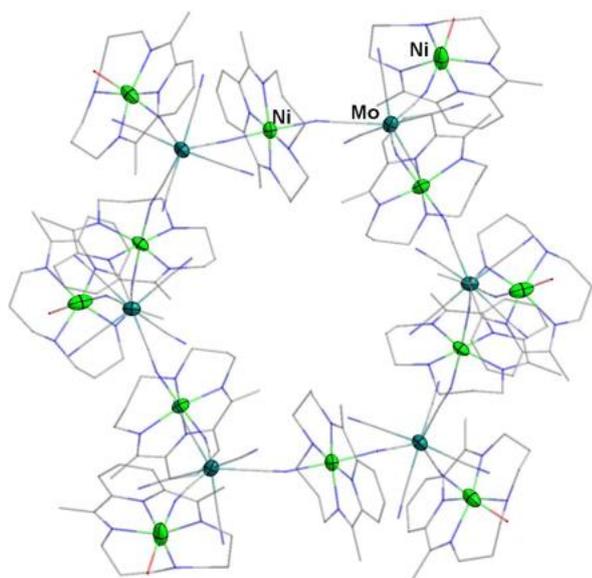
Figure 1. Structure of $\mathbf{Mo^{III}_6Ni_{12}}$. The nickel atoms are green, molybdenum atoms are teal, carbon atoms are grey, nitrogen atoms are blue, and oxygen atoms are red. Hydrogen atoms are omitted for the sake of clarity.

which crystallizes in $R\bar{3}$. The cell parameters of our new X-ray structure for $\mathbf{Mo^{IV}_6Ni_{12}}$ are smaller than those previously reported, consistent with the data being collected at 100 K rather than 273 K. We analyzed this structure in the rhombohedral setting in order to facilitate direct comparisons to the unit cell of $\mathbf{Mo^{III}_6Ni_{12}}$ (Table S4). Despite the structural similarities of the two molecules, lowering the symmetry by going from $[Mo^{IV}(CN)_8]^{4-}$ to $[Mo^{III}(CN)_7]^{4-}$ changes the crystal system from trigonal to primitive.

The molecule of $\mathbf{Mo^{III}_6Ni_{12}}$ resides on a crystallographic inversion center with one-half of the complex in the asymmetric unit (Figure S1). The structure consists of six $[Mo^{III}(CN)_7]^{4-}$ moieties bridged to six [Ni(L)] moieties in an alternating arrangement to give a wheel motif (Figure 1). The remaining six $[Ni(L)]^{2+}$ act as capping ligands for the wheel with one coordinated water in the Ni axial position opposite the cyanide ligand. The coordination geometry around the Mo^{III} centers was evaluated using the SHAPE program, which calculates a continuous shape measurement (CShM) based on the positions of the atoms relative to their positions in ideal geometries (closer to 0 is a better match).[35,36] The coordination geometries of the Mo centers are best described as capped trigonal prismatic. The Mo3 is a particularly good fit for that geometry and the results of those calculations are compiled in the SI (Table S4, Figure S2). The angles between the equatorial cyanide ligands range from 71.9(4)° to 76.4(3)°, which are close to the 72° for a perfect pentagon. OLEX2 was used to calculate a mean plane of the equatorial cyanide ligands on each Mo^{III} center in $\mathbf{Mo^{III}_6Ni_{12}}$; the rmsd values for each of those planes are 0.549, 0.535, and 0.579 for Mo1-Mo3, further showing that the cyanide ligands are distorted compared to a perfect pentagonal arrangement. The Ni^{II} centers all adopt an approximately octahedral geometry, with the four equatorial positions being occupied by the N atoms of L and the axial positions filled with either two cyanide ligands (for the Ni atoms in the ring), or one cyanide ligand and one water ligand (for the Ni atoms on the outside).

Due to the similarities in the crystal structures of $\mathbf{Mo^{III}_6Ni_{12}}$ and $\mathbf{Mo^{IV}_6Ni_{12}}$, as well as the propensity for $[Mo^{III}(CN)_7]^{4-}$ to disproportionate into $[Mo^{III}(CN)_6]^{3-}$ and $[Mo^{IV}(CN)_8]$,[4-10,29,37] we verified the purity of the bulk sample of $\mathbf{Mo^{III}_6Ni_{12}}$ using IR spectroscopy. With crystalline samples of both compounds in hand,
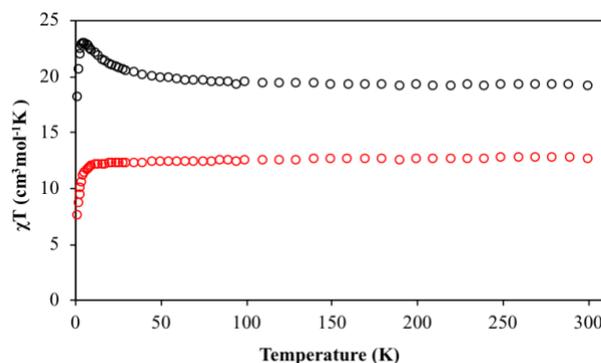
Figure 2. Magnetic susceptibilities of $\mathbf{Mo^{III}_6Ni_{12}}$ (black dots) and $\mathbf{Mo^{IV}_6Ni_{12}}$ (red dots).

we were able to compare the IR spectra of $\mathbf{Mo^{IV}_6Ni_{12}}$ and $\mathbf{Mo^{III}_6Ni_{12}}$ (Figure S3). Cyanide stretching frequencies in the spectrum of $\mathbf{Mo^{III}_6Ni_{12}}$ are located at 2092, 2079, 2044, and 2034 cm^{-1}. In the case of $\mathbf{Mo^{IV}_6Ni_{12}}$, the cyanide stretching frequencies occur at 2144, 2131, 2120, and 2100 cm^{-1}. Notably, no frequencies for $\mathbf{Mo^{IV}_6Ni_{12}}$ were observed in the spectrum of $\mathbf{Mo^{III}_6Ni_{12}}$, providing strong evidence that the compound is not a mixed valence compound possessing both $[Mo^{III}(CN)_7]^{4-}$ and $[Mo^{IV}(CN)_8]^{4-}$ anions in the structure. The red shift in the cyanide stretching frequencies of $\mathbf{Mo^{III}_6Ni_{12}}$ is consistent with a stronger π back-donation from Mo^{III} as compared to Mo^{IV}.

Being confident of the number of unpaired electrons on each metal center is obviously important for the interpretation of the magnetic data. Both capped trigonal prismatic geometry and distorted pentagonal bipyramidal geometry lead to distinct energy levels for each d orbital, forcing an $S = \frac{1}{2}$ ground state for each d^3 Mo^{III} center (Figure 4).[38] For $[Mo^{III}(CN)_7]^{4-}$, this distinction is particularly important because orbitally degenerate Mo^{III} centers have been conclusively shown to lead to anisotropic exchange.[31,32] In the absence of such degeneracy, isotropic coupling parameters are sufficient to understand the effect of coupling on the magnetic behavior of the molecule. The nickel centers are $S = 1$ in octahedral geometries.

Variable temperature static DC magnetic susceptibility measurements were performed on crushed crystals of $\mathbf{Mo^{III}_6Ni_{12}}$ from 300 to 2 K under an applied field of 1000 Oe (Figure 2). The room temperature $\chi_m T$ value of 19.07 cm^{3}mol^{-1}K is higher than the spin-only value of 14.25 cm^{3}mol^{-1}K ($g_{Mo}=2.0$, $S_{Mo} = \frac{1}{2}$, $g_{Ni} = 2.0$, $S_{Ni} = 1$) for the 18-metal center wheel. Calculations on seven-coordinate Mo^{III} centers have revealed that, even in distorted geometries, the g-values are highly anisotropic, with g_z ranging from 3.0 to 3.5 and $g_x = g_y$ ranging from 0.4 – 1.3.[31] Our calculations (*vide infra*) predict an average g_{iso} value between 2.23-2.24 for the Ni^{II} centers, which also has a substantial effect on $\chi_m T$. The observed room temperature $\chi_m T$ value is easily explained when accounting for these highly anisotropic g values (19.10 cm^{3}mol^{-1}K, $g_{Mo} = 1.80$, $S_{Mo} = \frac{1}{2}$, $g_{Ni} = 2.40$, $S_{Ni} = 1$). The $\chi_m T$ value increases from 19.07 cm^{3}mol^{-1}K at 300 K to a maximum of 22.92 cm^{3}mol^{-1}K at 5 K before dropping precipitously as the temperature is lowered to 2 K. We attribute the decrease in $\chi_m T$ at very low temperatures to zero-field splitting (zfs) of the Ni^{II} centers. The increase from 300 to 5 K is likely due to coupling between the Ni^{II} and Mo^{III} centers. In the case where one set of Ni-Mo couplings is ferromagnetic and another set is antiferromagnetic (this is possible when inner-ring six Ni^{II} and all Mo^{III} spins are parallel and the external six Ni^{II} centers are antiparallel), then $S = 3$ would be expected; the room temperature value of $\chi_m T$ rules out such a possibility, since $\chi_m T$ would be expected to be 6 cm^{3}mol^{-1}K in that case. Both fully antiferromagnetic ($S = 9$, $\chi_m T = 45$ cm^{3}mol^{-1}K, when all the Ni^{II} centers have a spin-up configuration and all the Mo^{III} have a spin-
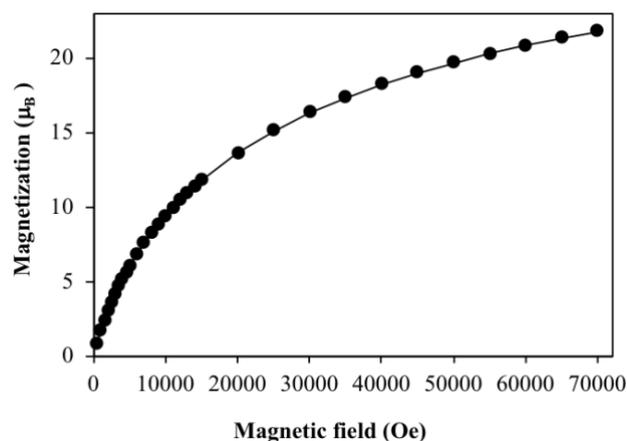
Figure 3. 1.8K magnetization for $\mathbf{Mo_6^{III}Ni_{12}}$. The solid black line is a guide for the eyes.

Figure 4. CASSCF-computed d-orbital ordering for Ni^{II} ions in $\mathbf{Mo_6^{III}Ni_{12}}$

down configuration) and fully ferromagnetic (S = 15, $\chi_m T$ = 120 $cm^3mol^{-1}K$, when all Ni^{II} and Mo^{III} centers have a spin-up configuration) coupling would lead to an increase in $\chi_m T$ at low temperatures. It is difficult to distinguish between the two based on the magnetic data alone, but the magnetization data and calculations lead us to believe that the coupling is ferromagnetic in nature (*vide infra*).

The magnetic susceptibility data for $\mathbf{Mo_6^{IV}Ni_{12}}$ reveal a value of 12.6 $cm^3mol^{-1}K$ at 300 K, which is close to the previously reported value of 12.19 $cm^3mol^{-1}K$ at 300 K.[25] We included our data for the magnetic susceptibility of $\mathbf{Mo_6^{IV}Ni_{12}}$ in Figure 2 to facilitate direct comparison of the magnetic properties, which clearly shows the differences in magnetic behavior. The number of metal centers present in $\mathbf{Mo_6^{III}Ni_{12}}$ precludes the use of complete models to fit the data. Our attempts based on previously reported methods[39] have not yielded satisfactory fits.

Dynamic AC measurements were performed, but no out-of-phase signal was observed even under applied DC fields up to 2000 Oe. which is in accord with the fact that the D_{5h} symmetry of the $[Mo^{III}(CN)_7]^{4-}$ anion has not been preserved.

The 1.8K magnetization data for $\mathbf{Mo_6^{III}Ni_{12}}$ (Figure 3) do not saturate up to a field of 7T, at which field the magnetization is 21.8 μ_B. The spin-only value predicted for an S = 9 ground state (antiferromagnetic coupling between Ni^{II} and Mo^{III}) is 18 μ_B, whereas the value predicted for S = 15 (ferromagnetic coupling) is 30 μ_B. Since there is a lack of saturation in the data, one would expect that the coupling is weakly ferromagnetic with the population of low-lying excited states. Calculations were performed to glean additional confirmation.

The exchange interactions between the metal centers and the magnetic anisotropy of Ni^{II} ions were evaluated using DFT and *ab initio* CASSCF calculations, respectively (See ESI for computational details). The entire complex is too large for computing the exchange interactions, therefore calculations were performed on one-half of the molecule $\{Mo^{III}_3Ni_6\}$ (Figure S5). Two isotropic coupling constants were computed, *viz.*, the magnetic interactions between the inner ring Ni^{II} ions and Mo^{III} ions labeled as the J_1 interaction and the interaction between the external Ni^{II} ions and Mo^{III} ions which is assigned as the J_2 interaction. The calculations predict that both J_1 and J_2 interactions are ferromagnetic in nature with the values of +20.5 and +8.3 cm^{-1}, respectively (Table S7). The ferromagnetic interaction values indicate that all Mo^{III} and Ni^{II} ions have spin-up configurations, leading to a ground state of S = 15. These calculated ferromagnetic interactions
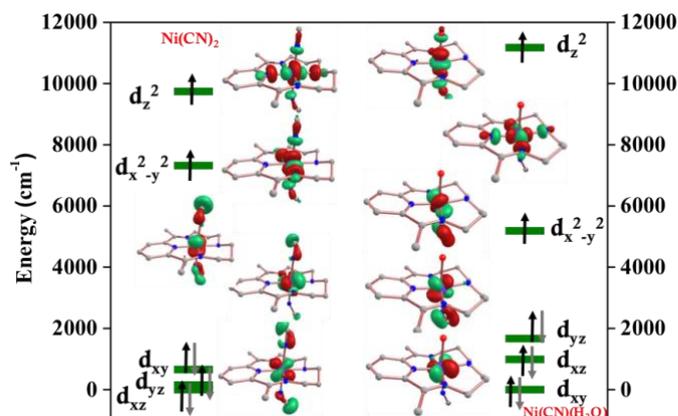
are consistent with reported exchange constants values between 4d/5d and Ni^{II} ions.[40,41]

Ab initio CASSCF calculations were performed to compute the zfs (*D*) of Ni ions and *g* parameters for both Ni and Mo ions in $\mathbf{Mo_6^{III}Ni_{12}}$. Calculations suggest a *g* value of 1.76 (g_x =1.03, g_y= 1.05 and g_z = 3.19) for $\{Mo^{III}CN_7\}$ center which is in close agreement with the reported values[31] and rationalizes the expected room temperature $\chi_m T$ value when considering anisotropic Ni centers (Figure S6 and Table S8). Calculations predict a negative *D* value (-6.2 cm^{-1}) and g = 2.23 for the inner ring Ni^{II} ions with two –CN groups in axial positions ($\{Ni(CN)_2\}$), and a positive *D* value (+11.2 cm^{-1}) and g = 2.24 for the external Ni^{II} ions with a H_2O molecule and a –CN group in their axial positions ($\{Ni(CN)(H_2O)\}$) (Figure S7 and Table S8). The computed crystal field splitting of the d orbitals for Ni^{II} ions are depicted in Figure 4. Based on the orbital splitting in the $\{Ni(CN)_2\}$ centers, the first excitation involves orbitals with the same $|\pm m_l|$ values (d_{xy} to d_{x2-y2}) resulting in a negative *D* value as expected. In contrast, for the $\{Ni(CN)(H_2O)\}$ centers, the first excitation occurs between the d_{xz} and d_{yz} orbitals (different $|\pm m_l|$ values) leading to a positive *D* value. In both cases, the major contribution to the *D* value arises from the triplet excited states (Table S9). The energy gaps between the ground and the first excited triplet states are relatively large, leading to either a small negative or positive D value.

This work demonstrates that syntheses of octacyanocyanometallate containing compounds can be extended to the heptacyano derivatives. By using $[Mo^{III}(CN)_7]^{4-}$ in this synthesis instead of $[Mo^{IV}(CN)_8]^{4-}$, an analogue was isolated that exhibits coupling between the Mo and Ni centers. The magnetic data and the calculations, taken together, provide strong evidence that the coupling is ferromagnetic in nature. This strategy can be useful in future work as a shortcut to reliably obtain new molecules that contain $[Mo^{III}(CN)_7]^{4-}$ which will expand the study of polynuclear cyanide bridged materials with unusual seven-coordinate coordination environments.

Conflicts of interest

The authors have no conflicts to declare.

Acknowledgements

Notes and references

1   R. Sessoli, D. Gatteschi, A. Canechi and M. A. Novak, *Nature*, 1993, **365**, 141-143.
2   S. Ferlay, T. Mallah, R. Ouahes, P. Veillet and M. Verdaguer, *Nature*, 1995, **378**, 701-703.
3   B. Sieklucka, R. Podgajny, D. Pinkowicz, B. Nowicka, T. Korzeniak, M. Balanda, T. Wasiutynski, R. Pelka, M. Makarewicz, M. Czapla, M. Rams, B. Gawel and W. Lasocha, *Cryst. Eng. Comm.*, 2009, **11**, 2032-2039.
4   X.-Y. Wang, C. Avendano and K. R. Dunbar, *Chem. Soc. Rev.*, 2011, **40**, 3213-3238.
5   K. S. Pedersen, J. Bendix and R. Clerac, *Chem. Commun.*, 2014, **50**, 4396-4415.
6   M. N. Leuenberger and D. Loss, *Nature*, 2001, **410**, 789-793.
7   G. A. Timco, S. Carretta, F. Troiani, F. Tuna, R. J. Pritchard, C. A. Muryn, E. J. L. McInnes, A. Ghirri, A. Candini, P. Santini, G. Amoretti, M. Affronte and R. E. P. Winpenny, *Nat. Nanotech.*, 2009, **4**, 173-178.
8   M. Feng and M. L. Tong, *Chem. Eur. J.*, 2018, **24**, 7574-7594.
9   J. M. Frost, K. L. M. Harriman and M. Murugesu, *Chem. Sci.*, 2016, **7**, 2470-2491.
10 D. Pinkowicz, H. Southerland, X.-Y. Wang and K. R. Dunbar, *J. Am. Chem. Soc.*, 2014, **136**, 9922-9924.
11 T. D. Harris, C. Coulon, R. Clérac and J. R. Long, *J. Am. Chem. Soc.*, 2011, **133**, 123-130.
12 X.-Y. Wang, A. V. Prosvirin and K. R. Dunbar, *Angew. Chem. Int. Ed.*, 2010, **49**, 5081-5084.
13 A.-A. H. Abu-Nawwas, J. Cano, P. Christian, T. Mallah, G. Rajaraman, S. J. Teat, R. E. P. Winpenny and Y. Yukawa, *Chem. Commun.*, 2004, **0**, 314-315.
14 M. Affronte, S. Carretta, G. A. Timco and R. E. P. Winpenny, *Chem. Commun.*, 2007, **0**, 1789-1797.
15 R. W. Saalfrank, A. Scheurer, R. Prakash, F. W. Heinemann, T. Nakajima, F. Hampel, R. Leppin, B. Pilawa, H. Rupp and P. Müller, *Inorg. Chem.*, 2007, **46**, 1586-1592.
16 N. Hoshino, A. M. Ako, A. K. Powell and H. Oshio, *Inorg. Chem.*, 2009, **48**, 3396-3407.
17 S. K. Langley, B. Moubaraki, C. M. Forsyth, I. A. Gass and K. S. Murray, *Dalton Trans.*, 2010, **39**, 1705-1708.
18 S. Muche, I. Levacheva, O. Samsonova, L. Pham, G. Christou, U. Bakowsky and M. Hołyńska, *Inorg. Chem.*, 2014, **53**, 7642-7649.
19 K. R. Vignesh, S. K. Langley, B. Moubaraki, K. S. Murray and G. Rajaraman, *Chem. Eur. J.*, 2015, **21**, 16364-16369.
20 Y. Huo, Y.-C. Chen, J.-L. Liu, J.-H. Jia, W.-B. Chen, S.-G. Wu and M.-L. Tong, *Dalton Trans.*, 2017, **46**, 16796-16801.
21 X.-Y. Zheng, Y.-H. Jiang, G.-L. Zhuang, D.-P. Liu, H.-G. Liao, X.-J. Kong, L.-S. Long and L.-S. Zheng, *J. Am. Chem. Soc.*, 2017, **139**, 18178-18181.
22 Z.-H. Ni, H.-Z. Kou, L.-F. Zhang, C. Ge, A.-L. Cui, R.-J. Wang, Y. Li and O. Sato, *Angew. Chem. Int. Ed.*, 2005, **44**, 7742-7745.
23 Z.-H. Ni, L.-F. Zhang, V. Tangoulis, W. Wernsdorfer, A.-L. Cui, O. Sato and H.-Z. Kou, *Inorg. Chem.*, 2007, **46**, 6029-6037.
24 Z. Ni, L. Zhang, A. Cui and H. Kou, *Sci. China, Ser. B: Chem.*, 2009, **52**, 1444-1450.
25 D. Zhang, L. Kong, H. Zhang and P. Wang, *Z. Naturforsch. B Chem. Sci.*, 2015, **70**, 527.
26 D.-P. Zhang, L.-F. Zhang, G.-L. Li and Z.-H. Ni, *Chem. Commun.*, 2013, **49**, 9582-9584.
27 R. Pradhan, C. Desplanches, P. Guionneau and J.-P. Sutter, *Inorg. Chem.*, 2003, **42**, 6607-6609.
28 J. Larionova, O. Kahn, S. Gohlen, L. Ouahab and R. Clérac, *J. Am. Chem. Soc.*, 1999, **121**, 3349-3356.
29 A. Kaur Sra, M. Andruh, O. Kahn, S. Golhen, L. Ouahab and J. V. Yakhmi, *Angew. Chem. Int. Ed.*, 1999, **38**, 2606-2609.
30 K. Qian, X.-C. Huang, C. Zhou, X.-Z. You, X.-Y. Wang and K. R. Dunbar, *J. Am. Chem. Soc.*, 2013, **135**, 13302-13305.
31 V. S. Mironov, L. F. Chibotaru and A. Ceulemans, *J. Am. Chem. Soc.*, 2003, **125**, 9750-9760.
32 V. S. Mironov, *Inorg. Chem.*, 2015, **54**, 11339-11355.
33 D.-Q. Wu, D. Shao, X.-Q. Wei, F.-X. Shen, L. Shi, D. Kempe, Y.-Z. Zhang, K. R. Dunbar and X.-Y. Wang, *J. Am. Chem. Soc.*, 2017, **139**, 11714-11717.
34 R. C. Young, *J. Am. Chem. Soc.*, 1932, **54**, 1402-1405.
35 S. Alvarez, P. Alemany, D. Casanova, J. Cirera, M. Llunell and D. Avnir, *Coord. Chem. Rev.*, 2005, **249**, 1693-1708.
36 M. Llunell, D. Casanova, J. Cirera, P. Alemany and S. Alvarez, SHAPE (version 2.1), Universitat de Barcelona, Barcelona, Spain, 2010.
37 X.-Y. Wang, M. G. Hilfiger, A. Prosvirin and K. R. Dunbar, *Chem. Commun.*, 2010, **46**, 4484-4486.
38 R. Hoffmann, B. F. Beier, E. L. Muetterties and A. R. Rossi, *Inorg. Chem.*, 1977, **16**, 511-522.
39 I.-R. Jeon and T. David Harris, *Chem. Commun.*, 2016, **52**, 1006-1008.
40 S. K. Singh, K. R. Vignesh, V. Archana and G. Rajaraman, *Dalton Trans.*, 2016, **45**, 8201-8214.
41 T. D. Harris, M. V. Bennett, R. Clérac and J. R. Long, *J. Am. Chem. Soc.*, 2010, **132**, 3980-3988.

A new, cyanide-bridged Mo_6Ni_{12} wheel shows ferromagnetic coupling.

$[Mo^{III}(CN)_7]_4[Ni(L)]_{12}(H_2O)_6$

$[Mo^{IV}(CN)_8]_6[Ni(L)]_{12}(H_2O)_6$